HHS Public Access

Author manuscript

Free Radic Biol Med. Author manuscript; available in PMC 2018 April 06.

Published in final edited form as:

Free Radic Biol Med. 2017 December ; 113: 48–58. doi:10.1016/j.freeradbiomed.2017.09.011.

Suppressed ubiquitination of Nrf2 by p47^{phox} contributes to Nrf2 activation

Kyun Ha Kim[a], **Ruxana T. Sadikot**[b], **Ji Yeon Lee**[a], **Han-Sol Jeong**[a], **Yu-Kyoung Oh**[c], **Timothy S. Blackwell**[d], and **Myungsoo Joo**[a,*]

[a]Division of Applied Medicine, School of Korean Medicine, Pusan National University, Yangsan 50612, Republic of Korea

[b]Section of Pulmonary and Critical Care Medicine, Atlanta Veterans Affairs Medical Center, Emory University, Decatur, GA 30033, USA

[c]College of Pharmacy and Research Institute of Pharmaceutical Sciences, Seoul National University, Seoul 08826, Republic of Korea

[d]Department of Medicine, Division of Allergy, Pulmonary and Critical Care Medicine, Vanderbilt University, Nashville, TN 37232, USA

Abstract

Although critical in phagocytosis in innate immunity, reactive oxygen species (ROS) collaterally inflict damage to host phagocytes because they indiscriminate targets. Since Nrf2 increases the expression of anti-oxidant enzymes that nullifies ROS, ROS activating Nrf2 is a critical negative regulatory step for countering the deleterious effects of ROS. Here, we postulate whether, along with ROS activating Nrf2, NADPH oxidase components also participate in direct activation of Nrf2, contributing to protection from ROS. Our results show that the p47^{phox} of the NADPH oxidase, but not p65^{phox} or p40^{phox}, physically binds to Nrf2, activating the Nrf2 function. p47^{phox} binding to Nrf2/Keap1 complex suppresses the ubiquitination of Nrf2, while p47^{phox} becomes ubiquitinated by Keap1. p47^{phox} increases the nuclear translocation of Nrf2 and the expression of Nrf2-dependent genes, whereas genetic ablation of p47^{phox} decreases the expression of those genes. In a lipopolysaccharide-induced acute lung inflammation mouse model, selective expression of p47^{phox} in mouse lungs induces the expression of Nrf2-dependent genes and is sufficient to suppress neutrophilic lung inflammation. Therefore, our findings suggest that p47^{phox} is a novel regulator of Nrf2 function.

Keywords

Nrf2; p47phox; NADPH oxidase; Keap1; Ubiquitination; Lung inflammation

*Corresponding author. mjoo@pusan.ac.kr (M. Joo).

Conflicts of interest

The authors declare no competing financial interest in relation to the study.

Appendix A. Supplementary material

Supplementary data associated with this article can be found in the online version at http://dx.doi.org/10.1016/j.freeradbiomed.2017.09.011.

1. Introduction

Macrophages and neutrophils are key effector cells in innate immunity [1–3], and reactive oxygen species (ROS) are a critical component for their effector function [4]. These phagocytic cells engulf invading bacteria in the form of the phagosome, where bacteria are bombarded by superoxide and other bactericidal ROS generated by NADPH oxidase [5, 6]. The importance of ROS in fending off bacterial infection is highlighted in patients with chronic granulomatous disease: the patients suffer from recurrent and life-threatening bacterial infections due to the lack of a functional NADPH oxidase [7]. While crucial in innate immunity, ROS can also cause harm by overwhelming the anti-oxidant system of host cells [8]. Excessive ROS result in oxidative stress and inflict ROS-mediated damages to key cellular constituents such as nucleic acid, lipids, and proteins, which are often associated with inflammation, carcinogenesis, neurodegeneration, aging, and other diseases [9–13]. Therefore, regulating ROS tightly is critical for the homeostasis of the innate immunity.

NADPH oxidase is the enzyme responsible for producing superoxide, a precursor molecule for bactericidal ROS [8]. In phagocytes, NADPH oxidase comprises the flavocytochrome b_{558} (cyt b_{558}) that consists of two membrane subunits (gp91^{phox}, or NOX2, and p22^{phox}) and four cytosolic subunits (p40^{phox}, p47^{phox}, p67^{phox}, and Rac) [14]. Among these subunits, NOX2 [15] and p47^{phox} [16] are highly expressed in myeloid cells including phagocytes. Myeloid-limited transcription factor PU.1 plays an important role in the transcription of NOX2 and p47^{phox} [17], although mRNA of NOX2 and p47^{phox} can be found in various tissues [18]. Upon stimulation by bacterial products or other inflammatory stimuli, these subunits are assembled on the membrane subunits, forming an active NADPH oxidase complex and producing superoxide and ROS.

ROS produced during phagocytosis tend to leak into the cytosol, initiating redox activity, which could yield harmful effect on the host cell [19]. ROS can be scavenged by activating Nrf2 because Nrf2, a basic leucine zipper transcription factor, regulates the expression of various phase 2 detoxification genes, such as glutamate-cysteine ligase catalytic subunit (GCLC), NAD(P)H:quinine oxidoreductase-1 (NQO1), and heme oxygenase-1 (HO-1) [20–23]. The activation of Nrf2 is achievable by inactivating Keap1, an inhibitor of Nrf2 [24]. In the normal condition, Keap1 dimer constantly recruits Nrf2 by binding to two different motifs on Nrf2, ETGE and DLG motifs [25]. This binding induces the ubiquitination of Nrf2, resulting in an ubiquitin-dependent degradation and thus a low level of Nrf2. When ROS are present, ROS modify the cysteine residues on Keap1, which weakens the interaction between Keap1 and the DLG motif of Nrf2, blocking Keap1-mediated ubiquitination of Nrf2 [26]. As a result, Nrf2 starts accumulated in the nucleus [27], binds to the cis-acting antioxidant response element (ARE) sequence, and induces the expression of the phase 2 detoxification genes [28]. Nrf2 is closely associated with suppressing inflammation, as evidenced in various inflammatory lung disease mouse models including acute lung injury (ALI) [29], chronic obstructive pulmonary disease (COPD) [30], asthma [31], and sepsis [32]. Therefore, Nrf2 plays an important role in the homeostasis of innate immunity.

Given that ROS can collaterally harm ROS-producing phagocytes, activation of Nrf2 is a critical measure for phagocytic cells to protect from ROS. Since NADPH oxidase is a key enzyme producing ROS in phagocytes and ROS activate Nrf2, we tested the possibility that the components in NOX2 NADPH oxidase in macrophages are also involved in activation of Nrf2, contributing further to minimizing the deleterious effects of ROS. To test this possibility, we examined whether Nrf2-Keap1 complex binds to NADPH oxidase subunits. Here, we provide evidence that $p47^{phox}$, but not $p67^{phox}$ or $p40^{phox}$, binds to and activates Nrf2, enhancing the function of Nrf2 in Suppressing inflammation.

2. Materials and methods

2.1. Cell culture and bone marrow-derived macrophages

A mouse macrophage cell line, RAW 264.7, and human embryonic kidney (HEK) 293 cells were purchased from American Type Culture Collection (Rockville, MD, USA). Cells were cultured in Dulbecco's Modified Eagle's Medium (DMEM) supplemented with L-glutamine (200 mg/L) (Hyclone; Logan, UT, USA), 10% (v/v) heat-inactivated fetal bovine serum (FBS; Sigma-Aldrich, Seoul, Korea), 100 U/ml penicillin, and 100 μg/ml streptomycin (Thermo Scientific, IL, USA). Bone marrow-derived macrophages (BMDM) were obtained from mice as described elsewhere [33]. In short, cellular materials of mouse femurs were flushed out with PBS and cultured in DMEM containing 10% FBS and 10% L929 cell culture medium for five days. Before the experiment, cells were maintained in a humidified incubator at 37 °C with 5% CO_2.

2.2. DNA constructs

V5-Nrf2 expression vector (pcDNA1/V5-Nrf2; a gift from Dr. YW Kan), Keap1 expression vectors (pcDNA3.1/Keap1 and pcDNA3.1/ FLAG-Keap1; gifts from Dr. ML Freeman), GST-Nrf2 (a gift from Dr. ML Freeman), and HA-ubiquitin expression vector (pMT123/HA-Ub; a gift from Dr. D Bohmann) were used for the study. Murine cDNA of $p47^{phox}$ with 3′ FLAG was amplified with 5′-GGGAATTCGCCATGGGGGACACCTTCATTCG-3′ and 5′-CCTCT AGAC TACTTATCGTCGTCATCCTTGTAATCCACAGCGGACGTCAGCTTC-3′. PCR product was inserted into a pCI-neo vector (Promega, Madison, WI, USA), yielding pCI-neo/ FLAG-$p47^{phox}$. $p47^{phox}$-PX that contains the N-terminal phagocyte oxidase domain was amplified by a pair of primers: 5′-CGAAGCTTTCACACAGCGGACGTCAGC-3′ and 5′-C CTCTAG ACTACTTATCGTCGTCATCCTTGTAATCTGTGATGTCAGCT ACGTTATTC-3′. $p47^{phox}$ -$SH3_A$/$SH3_B$ that has two Src homology 3 (SH3) domains and the C-terminal proline-rich domain was amplified by 5′-GGGAATTCGCCACCATGGGCCCCATCATCCTTCAGA C −3′ and 5′-CCTCTAGACTACT TATCGTCGTCATCCTTGTAATCAGCCTTCTGCAGAT ACATGGA −3′. $p47^{phox}$-$SH3_B$ that harbors the second SH3 and the C-terminal proline-rich domain was amplified by 5′-GGGAATTCGCCACCATGGGCCGCGGGGCACCACC-3′ and 5′-CCTCTAGACTACTTATCGTCGTCATCCTTGTAATCCACAGCGG ACGTCAGCT TC −3′. Nucleotide sequencing was performed to confirm each clone. All the plasmids used in this study were prepared with EndoFree plasmid kit (Qiagen, Hilden, Germany).

2.3. Cell lysate, immunoprecipitation, and western blot analysis

Total cell extracts were prepared by RIPA (Thermo Scientific) or NP-40 lysis buffer (50 mM Tris pH7.4, 150 mM NaCl, 1.5 mM EDTA, 3% Glycerol and 0.3% NP-40) with a protease inhibitors cocktail (Roche, Seoul, Korea). Nuclear proteins were isolated with NE-PER nuclear extraction kit and the manufacturer's protocol (Thermo Scientific). Proteins were quantified by the Bradford assay (Bio-Rad, Hercules, CA, USA) as specified by the manufacturer. For immunoprecipitation, 2 μg of antibodies were added to the cell lysate precleared with Pierce® protein A-sepharose (Thermo Fisher). After overnight incubation at 4 °C, immune complexes were captured with 50 μl of Pierce® protein A-Sepharose (Thermo Fisher) for 30 min at 4 °C. Proteins fractionated by SDS-PAGE were transferred to PVDF membrane (EMD Millipore, Billerica, MA, USA), which was incubated with appropriate antibodies. The proteins of interest were revealed by chemiluminescence (SuperSignal® West Femto, Thermo Scientific) Antibodies against Nrf2 (H-300), $p47^{phox}$ (H-195), $p67^{phox}$ (N-19), $p40^{phox}$ (D-8), NQO1 (C-1), HO-1 (U-19), β-actin (C-4), lamin A/C (H-110), and isotypic IgG were purchased from Santa Cruz Biotechnology (Santa Cruz, CA, USA). Antibodies against FLAG (F1804) and HA (H3663) and phorbol 12-myristate 13-acetate (PMA) were from Sigma-Aldrich, and antibodies against GCLC (RB-1697) and V5 (R960-25) were from Thermo Fisher.

2.4. GST-pull down assay

GST-Nrf2 was expressed in *E. coli* DH5α as instructed by the manufacturer (Promega). GST-Nrf2 captured by Pierce™ Glutathione (GSH) agarose (Thermo Fisher) was incubated with cell lysate that contained the FLAG-tagged full-length or deletion mutants of $p47^{phox}$. The beads were washed three times with the cell lysis buffer (Thermo Fisher) with 250 mM NaCl. Bound proteins were analyzed by immunoblotting for FLAG.

2.5. Ubiquitination assay

HEK 293 cells were transfected with expression vectors of HA-Ub, V5-Nrf2, FLAG-Keap1, and FLAG-$p47^{phox}$. At 24 h after transfection, the transfected cells were treated with ten μM MG132 (Sigma-Aldrich) for three h. Cell extracts were prepared, to which antibodies were added for immunoprecipitation. The immune complex was captured with Pierce® protein A-sepharose (Thermo Fisher) and analyzed by immunoblotting for ubiquitin.

2.6. Reporter cells and assay

RAW 264.7 cells were stably transfected with a Nrf2 reporter vector that contains a 1-kb long promoter of NQO-1 harboring ARE in pGL4.17[luc2/Neo (Promega). The reporter cell line was transiently transfected with V5-Nrf2 and $p47^{phox}$ expressing vectors. At 24 h after transfection, luciferase activity was measured with a luciferase assay kit (Promega) per the manufacturer's protocol. Luciferase activity was normalized with the amounts of proteins in each cell lysate.

2.7. Total RNA extraction, semi-quantitative RT-PCR, and real-time quantitative PCR

Total RNA was isolated with the QIAGEN RNeasy® mini kit (Qiagen) and the instructions. Two μg of RNA was reverse-transcribed by M-MLV reverse transcriptase (Promega) to

generate cDNA. The quantity of each mRNA was determined by using end-point dilution PCR, including three serial 1–5 dilutions (1:1, 1:5, 1:25, and 1:125) of RT products before PCR amplification. For eliminating genomic DNA contamination, equal amounts of total RNA of each sample were PCR amplified without RT reaction. cDNA was amplified by PCR with a set of specific primers: the forward and the reverse primers for NQO-1 were 5′-GCAG TGCTTTCCATCACCAC-3′ and 5′-TGGAGTGTGCCCAATGCTAT-3′; the primers for HO-1 were 5′-TGAAGGAGGCCACCAAGGAGG-3′ and 5′-AGAGGTCACCCAGGTAGCGG G-3′; the primers for GCLC were 5′-CACTGCCAGAACACAGACCC-3′ and 5′-ATGGTCT GGCTGAGAAGCCT-3′; and the primers for GAPDH were 5′-GGAGCCAAAAGGGTCAT CAT-3′ and 5′-GTGATGGCATGGACTGTGGT-3′. *Taq*PCRx DNA polymerase (Thermo Fisher) and the manufacturer's protocol were used for PCR. The reaction conditions were as follows: an initial denaturation at 95 °C for 5 min followed by 25 cycles of denaturation for 30 s at 95 °C, annealing for 30 s at 55 °C, and extension for 40 s at 72 °C with a final extension for 7 min at 72 °C. Amplicons were separated on 1.5% agarose gels in 1× TBE buffer, stained with GRgreen (Biolabo, châtel-St-Denis, Switzerland), and visualized under LED light. GAPDH (Glyceraldehyde-3-phosphate dehydrogenase) was used as internal controls to evaluate relative expressions of NQO-1, GCLC, and HO-1. For real-time qPCR, 1 μg of total RNA was reverse-transcribed as described above. PCR amplification was performed using an SYBR Green premixed Taq reaction mixture with gene-specific primers. The forward and reverse primers for NQO-1 were 5′-GCATAGAGGTCCGACTCCAC-3′ and 5′-GGACTGCACCAGAGCCAT-3′; the primers for GCLC were 5′-GTCCTTTCCCCCTTC TCTTG-3′ and 5′-AGGACGTTCTCAAGTGGGG-3′; the primers for HO-1 were 5′-GGCTT CCCTCTGGGAGTCT-3′ and 5′-AGCTGCTGACCCATGACAC-3′; and the primers for glyceraldehyde-3-phosphate dehydrogenase (GAPDH) were 5′-TTAAAAGCAGCCCTGGT GAC-3′ and 5′-CT CTGCTCCTCCTGTTCGAC-3′. The PCR thermal cycling conditions consisted of 95 °C for 10 min, followed by 40cycles of 95 °C for 10 s, 57 °C for 15 s and 72 °C for 20 s. Real-time PCR was conducted using a Rotor-Gene Q real-time PCR system (Qiagen) with SYBR Green PCR Master Mix (Enzynomics). The threshold cycles (Ct) were used to quantify the mRNA expression of the target genes.

2.8. Animal model

Littermate wild-type (C57BL/6) and $p47^{phox\ -/-}$ mice were purchased from the Jackson Laboratory (Bar Harbor, Maine, U.S.A.) and inbred in a specific pathogen-free (SPF) facility at Pusan National University, Yangsan, Korea. Animals were housed in certified, standard laboratory cages, and fed with food and water ad libitum before the experiment. Male mice 7–10 weeks old) were used for the study. All experimental procedures followed the NIH of Korea Guidelines for the Care and Use of Laboratory Animals, and all experiment was approved by the Institutional Animal Care and Use Committee of Pusan National University (approval number: PNU-2010-00028). Mice were anesthetized by Zoletil (Virbac Korea, Seoul, Korea). $p47^{phox}$ expressing plasmid or pcDNA3.1 (1.5 mg/kg body weight) was mixed with EC10, a liposome that is engineered to carry DNA to the lung [34], which was loaded in MicroSprayer® Aerosolizer-Model IA-1C (Penn-Century, Wyndmoor, PA, USA) and then delivered in aerosol to the lung via trachea under visual guidance. Mice subsequently received a single intraperitoneal (i.p.) *E. coli* lipopolysaccharide (LPS)

(serotype 055:B5, 10 mg/kg body weight). At 24 h after LPS treatment, mice were sacrificed for analyses. Bilateral bronchoalveolar lavage (BAL) was performed as described elsewhere [35]. Total cells in BAL fluid were counted with a hemocytometer, and the cells in BAL fluid were stained for the differential counting of macrophages, lymphocytes, or neutrophils by Hemacolor (Merck, Darmstadt, Germany). Three hundred cells in total were counted, and one hundred of the cells in each microscopic field were scored. The mean number of cells per field was reported.

For collecting lung tissue, mouse lungs were perfused with saline and inflated with fixatives. After paraffin embedding, 5 μm sections were cut, placed on charged slides, and stained with a hematoxylin and eosin (HE) staining method. Three separate HE-stained sections were evaluated in 100× microscopic magnifications per mouse.

2.9. Statistical analysis

Statistical analysis of results was performed using PASW Statistics Data Editor v18 Korean, SPSS Inc, Chicago, IL, USA. Values are expressed as the mean ± SEM. Student's *t*-test and one-way analysis of variance (ANOVA) test with Tukey's post hoc test were applied for comparison of the means. *P* values < .05 were considered significant. All experiments were performed at least three times independently.

3. Results

3.1. $p47^{phox}$ of NADPH oxidase binds to Nrf2 in macrophages

We tested the possibility that NADPH oxidase complex regulates Nrf2 function via a direct physical interaction. Since the cytosolic subunits of the NADPH oxidase are likely candidates for the binding, we started with examining a possible binding between Nrf2 and $p47^{phox}$, the key factor that initiates the assembly of NADPH oxidase. The cytosolic fraction of RAW 264.7 cells was prepared, to which anti-$p47^{phox}$ antibody was added. Immune complexes formed by the anti-$p47^{phox}$ antibody were analyzed by immunoblotting for Nrf2. As shown in Fig. 1A, the anti-$p47^{phox}$ antibody precipitated Nrf2, while isotype IgG did not. To test whether two other major cytosolic subunits of NADPH oxidase also physically interact with Nrf2, we performed similar experiments. As shown in Fig. 1B and Fig. 1C, neither anti-$p67^{phox}$ antibody nor anti-$p40^{phox}$ antibody precipitated Nrf2. These results suggest that $p47^{phox}$, but not $p67^{phox}$ and $p40^{phox}$, physically binds to Nrf2.

To confirm the binding of Nrf2 with $p47^{phox}$, we took HEK 293 cells that lack intrinsic $p47^{phox}$ [15, 18], and transfected them with the plasmids encoding V5-Nrf2 and $p47^{phox}$. At 48 h after transfection, the cytosol of the transfected cells was prepared, to which anti-$p47^{phox}$ antibody was added. Immune complexes were analyzed by immunoblotting for V5-Nrf2. As shown in Fig. 1D, anti-$p47^{phox}$ antibody, but not isotypic IgG, precipitated Nrf2 (lanes 4, 5 and 6). Treatment of the transfected cells with PMA, which phosphorylates $p47^{phox}$, appeared not to affect the binding between the two proteins significantly (lanes 5 and 6). Nevertheless, these results show that $p47^{phox}$ physically bound to Nrf2.

3.2. PX and $SH3_A$ domains of $p47^{phox}$ mediate the binding to Nrf2

To further confirm the binding between Nrf2 with $p47^{phox}$, we performed GST-pull down assays. A full-length murine Nrf2 fused to GST was produced in *E. coli*, which was captured by GSH-beads. Then the GST-Nrf2 beads were incubated with the lysate of HEK293 cells transfected with FLAG-tagged $p47^{phox}$. Precipitated immune complexes were analyzed by immunoblotting for FLAG-tagged proteins. As shown in Fig. 2A, GST-Nrf2 precipitated $p47^{phox}$, confirming the physical interaction between $p47^{phox}$ and Nrf2.

Next, we located the domain on $p47^{phox}$ that is involved in binding to Nrf2. Since $p47^{phox}$ is composed of at least three distinctive domains, we created FLAG-tagged, deletion mutants of $p47^{phox}$ as follows (Fig. 2C): $p47^{phox}$-PX that contains N-terminal phagocyte oxidase domain, $p47^{phox}$-$SH3_A$/$SH3_B$ that has two Src homology 3 (SH3) domains and C-terminal proline-rich domain, and $p47^{phox}$-$SH3_B$ that harbors the second SH3 domain and the C-terminal proline-rich domain [36]. HEK293 cells were transfected with the plasmids encoding these mutants of $p47^{phox}$, and GST-Nrf2 pull-down assay was performed as described above. The mutants of $p47^{phox}$ that bound to GST-Nrf2 were analyzed by immunoblotting with the anti-FLAG antibody. As shown in Fig. 2B, Nrf2 bound to $p47^{phox}$-PX and $p47^{phox}$-$SH3_A$/$SH3_B$, but not to $p47^{phox}$-$SH3_B$. As summarized in schematics (Fig. 2C), these results suggest that the PX and the first SH3 domain ($SH3_A$) domains in $p47^{phox}$ mediate the physical interaction with Nrf2.

3.3. $p47^{phox}$ binding to the Nrf2/Keap1 complex results in $p47^{phox}$ ubiquitination

Since Nrf2 forms a complex with Keap1 in the cytoplasm [20], we tested whether $p47^{phox}$ affects the interaction between Nrf2 and Keap1. HEK 293 cells were transfected with plasmids encoding V5-Nrf2, FLAG-Keap1, and FLAG-$p47^{phox}$. The cytosolic fraction of the transfected cells was prepared and added with the anti-V5 antibody to precipitate Nrf2. Immune complexes formed by the anti-V5 antibody were analyzed by immunoblotting of FLAG-tagged proteins (Keap1 and $p47^{phox}$). As shown in Fig. 3A, Nrf2 precipitated Keap1, suggesting a robust binding between Nrf2 and Keap1 (lane 3). When $p47^{phox}$ was expressed along with Nrf2 and Keap1, the level of Keap1 precipitated by Nrf2 was not changed (lanes 3 and 4). Even a higher amount of $p47^{phox}$ did not alter the level of Keap1 precipitated (lanes 3 and 5). Conversely, Keap1 did not appear to affect the binding between Nrf2 and $p47^{phox}$ because the level of $p47^{phox}$ precipitated without co-transfection of Keap1 was similar to that with co-transfection of Keap1 (lanes 4, 5, 6 and 7). To confirm the interaction among $p47^{phox}$, Nrf2, and Keap1, we precipitated $p47^{phox}$ by adding an anti-$p47^{phox}$ antibody to the cell lysate, which was analyzed by immunoblotting for V5 (Nrf2) and FLAG (Keap1 and $p47^{phox}$). As shown in Fig. 3B, the precipitant formed by the anti-$p47^{phox}$ antibody contained V5-Nrf2 (top panel) and FLAG-Keap1 (second panel), suggesting that $p47^{phox}$ binds to Nrf2/Keap1 complex. To exclude the possibility of direct binding between $p47^{phox}$ and Keap1, we transfected HEK293 cells with plasmids encoding $p47^{phox}$ and FLAG-Keap1. The anti-$p47^{phox}$ antibody was added to the cytosol of the transfected cells, and immune complexes were analyzed by immunoblotting for FLAG (Keap1). As shown in Fig. 3C, the antibody against $p47^{phox}$ did not precipitate Keap1. These results suggest that $p47^{phox}$ binding to Nrf2 does not perturb the interaction between Nrf2 and Keap1.

Since Keap1 mediates ubiquitination of Nrf2 [20, 37] and, as shown above, $p47^{phox}$ formed a complex with Nrf2/Keap1 via Nrf2, we tested whether Keap1 ubiquitinates $p47^{phox}$. HEK 293 cells were transfected with plasmids encoding V5-Nrf2, HA-Ub, and Keap1, along with increasing amounts of FLAG-$p47^{phox}$ in the presence of MG132, a proteasome inhibitor that prevents ubiquitin-mediated protein degradation. The cytosolic proteins were prepared, and $p47^{phox}$ was precipitated by the anti-FLAG antibody and analyzed by immunoblotting for Ub to reveal ubiquitinated $p47^{phox}$. As shown in Fig. 3D, $p47^{phox}$ became ubiquitinated, which appears to increase as the amounts of transfected $p47^{phox}$ increased (lanes 2, 3 and 4). In contrast, ubiquitination of $p47^{phox}$ was not detectable in the absence of Keap1 (lane 5). These results suggest that $p47^{phox}$ can be ubiquitinated by Keap1 in the Nrf2/Keap1 complex. Collectively, these results suggest that $p47^{phox}$ binds to Nrf2/Keap 1 complex, which results in the ubiquitination of $p47^{phox}$.

3.4. $p47^{phox}$ suppresses the ubiquitination of Nrf2, increasing the level of nuclear Nrf2

Given that Keap1 ubiquitinated both Nrf2 and $p47^{phox}$ as shown above, we examined whether $p47^{phox}$ binding to Nrf2 affects the ubiquitination of Nrf2 by Keap1. HEK 293 cells were transfected with plasmids encoding V5-Nrf2, FLAG-Keap1, HA-Ubiquitin (Ub), and FLAG-$p47^{phox}$ in the presence and absence of MG132. V5-Nrf2 in the cytoplasm was precipitated by the anti-V5 antibody, which was analyzed by immunoblotting for HA-Ub to reveal ubiquitinated Nrf2. As shown in Fig. 4A, ubiquitination of Nrf2 was evident in the presence of Keap1 and MG132 (lane 2), which was decreased by $p47^{phox}$ (lane 3), suggesting that $p47^{phox}$ interferes with the ubiquitination of Nrf2. Since decreased ubiquitination of Nrf2 is closely associated with increased accumulation of Nrf2 in the nucleus, indicative of activated Nrf2, we examined whether the expression of $p47^{phox}$ results in the increase of the nuclear Nrf2. HEK 293 cells were similarly transfected with the plasmids, and the cytosolic and nuclear fractions of the transfected cells were prepared and analyzed by immunoblotting for V5-Nrf2. As shown in Fig. 4B, the transfected Nrf2 was found in the cytosolic fraction (lane 1, the top panel) as well as in the nucleus (lane 1, the 4th panel). When $p47^{phox}$ was over-expressed along with Nrf2, the levels of nuclear Nrf2 were increased (lane 2, the 4th panel), with a concomitant decrease of the cytosolic Nrf2 (lane 2, the 1st panel). The effect of $p47^{phox}$ on the nuclear Nrf2 was evident when a higher amount of $p47^{phox}$ was transfected (lane 3, the 1st and 4th panels). Densitometric analyses reveal that the levels of Nrf2 in the cytosol were changed inverse to those in the nucleus as the expression of $p47^{phox}$ increased (Fig. 4C). Together, these results suggest that $p47^{phox}$ suppresses the ubiquitination of Nrf2, resulting in Nrf2 accumulated in the nucleus.

3.5. $p47^{phox}$ enhances the expression of Nrf2 dependent genes in macrophages

Blocking the ubiquitination of Nrf2 results in the activation of Nrf2 and the induction of Nrf2 dependent gene expression [27]. Given our results showing that $p47^{phox}$ interfered with the ubiquitination of Nrf2 and induced the accumulation of nuclear Nrf2, we examined whether $p47^{phox}$ increases the transcriptional activity of Nrf2. We took Nrf2-luciferase reporter cells, which were derived from RAW 264.7 cells, and transfected them with a fixed amount of the Nrf2 expressing plasmid, along with increasing amounts of the $p47^{phox}$ expressing plasmid. At 48 h after transfection, cell lysate was prepared for luciferase assay. As shown in Fig. 5A, Nrf2 expressed by transfection induced luciferase activity, which was

further increased by $p47^{phox}$. To confirm this result, we examined whether the expression of $p47^{phox}$ results in the expression of Nrf2-dependent genes such as HO-1, GCLC, and NQO-1. HEK 293 cells were transfected with the Nrf2 expressing plasmid, along with increasing amounts of the $p47^{phox}$ expressing plasmid. Total RNA extracted from the transfected cells was analyzed by a real-time qPCR for those Nrf2-dependent genes. As shown in Fig. 5B, Nrf2 induced the expression of the Nrf2-dependent genes (2nd columns in each panel), which was significantly enhanced by $p47^{phox}$ (4th and 5th columns in each panel). These results suggest that $p47^{phox}$ enhances the transcriptional activity of Nrf2.

Given our result that $p47^{phox}$ enhanced the expression of Nrf2-de-pendent genes, it is likely that Nrf2-dependent gene expression is less robust when $p47^{phox}$ lacks. To test this possibility, we prepared bone marrow-derived macrophages (BMDM) from $p47^{phox-/-}$ mice and treated BMDM with sulforaphane to selectively activate Nrf2 [38]. Total proteins were extracted from the cells and analyzed by western blot. As shown in Fig. 6A, while sulforaphane induced the robust expression of HO-1, NQO-1, and GCLC in BMDM of wild-type (WT) mice (lane 2), similar treatment of BMDM of $p47^{phox-/-}$ mice induced those proteins in a lesser degree (lane 4). Densitometric analysis showed that the expression of those Nrf2-dependent genes in BMDM of $p47^{phox-/-}$ mice was significantly less than WT (Fig. 6B). Together, these results suggest that $p47^{phox}$ enhances the transcriptional activity of Nrf2, resulting in increased expression of Nrf2-dependent genes.

3.6. Expression of $p47^{phox}$ is sufficient to protect mice from LPS-induced lung inflammation

Since Nrf2 is a key factor that protects mice from various inflammatory lung diseases including ALI [29], we tested whether expression of $p47^{phox}$ in mouse lungs increases the activity of Nrf2, suppressing lung inflammation. First, we examined whether the expression of $p47^{phox}$ results in the activation of Nrf2 in mouse lungs. Mice (n = 5 per group) received three intratracheal (i.t.) deliveries of the plasmid expressing FLAG-$p47^{phox}$ or a host vector (pCI-neo). Two days after the administration, mouse lungs were harvested for extracting total RNA, and the expression of Nrf2-dependent genes was analyzed by semi-quantitative RT-PCR. As shown in Fig. 7A, delivery of $p47^{phox}$ to the lung increased the expressions of Nrf2-dependent genes such as HO-1, NQO-1, and GCLC in mouse lungs. Next, we examined whether $p47^{phox}$ suppresses lung inflammation (Fig. 7B). Similar to Fig. 7A, mice (n = 5 per group) received the FLAG-$p47^{phox}$ plasmid (b and d) or pCI-neo vector plasmid (a and c) before an intranasal (i.n.) LPS (c and d). At 24 h after LPS administration, mouse lungs were harvested for assessing the effect of $p47^{phox}$ on lung inflammation. Histologic analyses of lung tissue (Fig. 7B) show that a single i.n. LPS administration elicited inflammation (c), which was suppressed by $p47^{phox}$ delivered to the mouse lungs (d), suggesting that $p47^{phox}$ suppresses lung inflammation. To confirm the anti-inflammatory effect of $p47^{phox}$, we performed bronchoalveolar lavage (BAL) and differential counting of inflammatory cells in BAL fluid. Results show that $p47^{phox}$ delivered to the lung significantly suppressed LPS- induced cellular infiltration (Fig. 7C) and neutrophil infiltration (Fig. 7D). To further confirm $p47^{phox}$ suppressing neutrophil infiltration, we measured the enzymatic activity of MPO, a key enzyme found in neutrophils [39]. As shown in Fig. 7E, the single i.n. LPS increased MPO activity, which was significantly suppressed

by $p47^{phox}$. Together, these results show that expression of $p47^{phox}$ in mouse lungs increased the transcriptional activity of Nrf2 and suppressed neutrophilic lung inflammation, suggesting that $p47^{phox}$ increasing the activity of Nrf2 is associated with suppressed neutrophilic lung inflammation in mice.

4. Discussion

While serving as a key arsenal of phagocytes in fending off invading bacteria and other infectious pathogens [8], ROS can cause tissue damage by overwhelming the anti-oxidant system of host cells. Thus, a tight regulation of ROS is paramount for the homeostasis of innate immunity. In this study, we postulated that NADPH oxidase directly activates the Nrf2 function to regulate ROS. To test this hypothesis, we examined whether Nrf2/Keap1 interacts with the cytosolic subunits of NADPH oxidase in macrophages. Our results show that $p47^{phox}$, but not $p67^{phox}$ or $p40^{phox}$, physically bound to Nrf2. While being ubiquitinated by Keap1, $p47^{phox}$ suppressed the ubiquitination of Nrf2, increasing the level of the nuclear Nrf2 and inducing the expression of Nrf2-dependent genes. Consistent with $p47^{phox}$ enhancing Nrf2 activity, selective expression of $p47^{phox}$ in mouse lungs enhanced the expression of Nrf2-dependent genes and suppressed LPS-induced neutrophilic lung inflammation. Conversely, $p47^{phox-/-}$ mice showed a decreased expression of Nrf2-dependent genes, compared to WT mice. Therefore, our results suggest that $p47^{phox}$, one of the cytosolic subunits of NADPH oxidase, binds to Nrf2, resulting in suppressed ubiquitination of Nrf2 and thus enhancing the function of Nrf2.

The properties and functions of the subunits comprising the NADPH oxidase complex have been well documented [15, 36]. In unstimulated conditions, $p47^{phox}$, $p67^{phox}$, and $p40^{phox}$ form a trimeric complex in the cytoplasm [40]. Upon bacterial infection, $p47^{phox}$ becomes phosphorylated and carries $p67^{phox}$ and $p40^{phox}$ to cyt b_{558}, where Rac migrates to without the help of other factors, forming an active NADPH oxidase complex [18, 41, 42]. Therefore, given the interaction between $p47^{phox}$ and Nrf2, as shown in this study, one can presume that precipitating $p67^{phox}$ also brings down Nrf2 via $p47^{phox}$. However, we could not detect Nrf2 when precipitating $p67^{phox}$. While we cannot exclude the possibility that our experimental conditions for immunoprecipitation assays precluded the co-precipitation of other factors, this result suggests a possibility that a singleton $p47^{phox}$ engages in binding to Nrf2. In support of this notion, there is evidence that $p47^{phox}$ remains as a singleton without forming a trimer with $p67^{phox}$ and $p40^{phox}$ [43]. In addition, whether $p47^{phox}$ is a component of the active NADPH oxidase remains controversial because recent evidence shows that $p47^{phox}$ does not stay at the NADPH oxidase complex on the membrane [44]. This result suggests that while critical for assembling the NADPH oxidase complex, $p47^{phox}$ is dispensable for NADPH oxidase enzymatic activity per se. In addition, our results indicate that the phosphorylation status of $p47^{phox}$ might not be critical for $p47^{phox}$ to bind to Nrf2. Combined with results published by other groups, our findings suggest the likelihood that a group of singleton $p47^{phox}$ is involved in binding to Nrf2.

To confirm the binding between $p47^{phox}$ and Nrf2, we located the site on $p47^{phox}$ that engaged in binding to Nrf2. $p47^{phox}$ consists of PX, tandem SH3 ($SH3_A$ and $SH3_B$), polybasic, and C-terminal proline-rich domains [15, 36]. The PX domain is important in

binding to lipid in the membrane and moesin of cytoskeleton. While the tandem SH3 domain is involved in binding to the membrane component, $p22^{phox}$, the same domain binds to the polybasic domain for auto-inhibition of $p47^{phox}$ in a resting, unstimulated state, which suppresses the translocation of $p47^{phox}$ to cyt b_{558} in the membrane [15, 36]. On the other hand, the C-terminal proline-rich domain is important in forming a complex with $p67^{phox}$ [15, 36]. Our results show that both the PX domain and the first SH3 ($SH3_A$) of the tandem SH3 domain in $p47^{phox}$ were involved in binding to Nrf2, suggesting that a group of $p47^{phox}$, in which the PX domain and the first SH3 in the tandem SH3 domain are free, is eligible for the binding with Nrf2. Considering the incomplete understanding of whether or not $p47^{phox}$ exists as a trimeric form or a singleton and the available PX domain of $p47^{phox}$ in unstimulated conditions, our results suggest that $p47^{phox}$ physically binds to Nrf2 within cells.

Ubiquitination is one of the key mechanisms that regulate Nrf2 function, in which Keap1 plays a critical role [24, 27]. In normal conditions, Keap1 mediates ubiquitination of Nrf2 that is constantly synthesized. As a result, Nrf2 undergoes constant, ubiquitin-mediated degradation so that the level of Nrf2 is low in the nucleus. In oxidative environments, however, ROS make Keap1 dysfunctional by forming an adduct to Keap1, which interrupts the ubiquitination of Nrf2, resulting in the accumulation of Nrf2 in the nucleus. Our results show that, like ROS, $p47^{phox}$ suppressed the ubiquitination of Nrf2, increasing the nuclear Nrf2. Unlike ROS, however, $p47^{phox}$ became subject to ubiquitination by Keap1, instead of inactivating Keap1. Since no direct binding between $p47^{phox}$ and Keap1 was apparent, ubiquitination of $p47^{phox}$ by Keap1 is likely through $p47^{phox}$ binding to Nrf2. These results suggest the possibility that $p47^{phox}$ interferes with the ubiquitination of Nrf2 by diverting Keap1 activity towards itself, enhancing the anti-inflammatory function of Nrf2. In line with these results, transfection of $p47^{phox}$ into cells increased the nuclear localization of Nrf2 and induced the expression of Nrf2-dependent genes. Furthermore, when delivered to the mouse lung, $p47^{phox}$ induced the expression of Nrf2-dependent genes in the lung, which was sufficient to suppress neutrophilic lung inflammation in an LPS-induced ALI mouse model. These results suggest that $p47^{phox}$ impacts on the anti-inflammatory function of Nrf2, at least in part, via interrupting the ubiquitination of Nrf2 by Keap1.

It seems likely that, in normal conditions, a small population of $p47^{phox}$ engages in binding to Nrf2, because precipitating V5-Nrf2 with the anti-V5 antibody brought down a small amount of $p47^{phox}$, regardless of the amount of transfected $p47^{phox}$. When Nrf2 was activated by sulforaphane, which does not induce ROS production (data not shown) and thus excludes indirect activation of Nrf2 via ROS, the expression levels of Nrf2-dependent gene products, such as NQO-1, HO-1, and GCLC, in the BMDM of $p47^{phox-/-}$ were slightly less than those of WT, which was statistically significant reduction though. These results suggest that a group of singleton $p47^{phox}$ constantly binds to and activates Nrf2. The expression of $p47^{phox}$ is highly expressed in phagocytic cells [16], whereas Nrf2 is ubiquitously expressed [45]. Given that phagocytes endure the surge of ROS during phagocytosis, it would be plausible that $p47^{phox}$, which expresses mainly in phagocytic cells, contributes to a low-degree activation of Nrf2 in phagocytes, which makes the cells cope with the surge of ROS more effectively, compared with non-phagocytic cells.

In this study, we present evidence that $p47^{phox}$ physically binds to Nrf2, suppressing ubiquitination of Nrf2, which results in the enhanced transcriptional activity of Nrf2 in macrophages and mouse lungs. We also show that expression of $p47^{phox}$ in mouse lungs induced the Nrf2-dependent gene expression and protected mice from LPS-challenged neutrophilic lung inflammation. We propose a novel function of $p47^{phox}$ as a regulating factor for the anti-inflammatory activity of Nrf2.

Acknowledgments

We thank Dr. Michael Freeman at Vanderbilt University School of Medicine for the generous support for this study.

Funding

This work was supported by the National Research Foundation of Korea (NRF) grant funded by the Korea government (MSIP) (2014R1A5A2009936).

References

1. Thepen T, van Rooijen N, Kraal G. Alveolar macrophage elimination in vivo is associated with an increase in pulmonary immune response in mice. J. Exp. Med. 1989; 170(2):499–509. [PubMed: 2526847]
2. Hunter M, Wang Y, Eubank T, Baran C, Nana-Sinkam P, Marsh C. Survival of monocytes and macrophages and their role in health and disease. Front. Biosci. 2009; 14:4079–4102.
3. Abraham E, Carmody A, Shenkar R, Arcaroli J. Neutrophils as early immunologic effectors in hemorrhage- or endotoxemia-induced acute lung injury. Am. J. Physiol. Lung Cell. Mol. Physiol. 2000; 279(6):L1137–L1145. [PubMed: 11076804]
4. Cathcart MK. Regulation of superoxide anion production by NADPH oxidase in monocytes/macrophages: contributions to atherosclerosis. Arteriosclerosis Thromb. Vascu. 2004; 24(1):23–28.
5. Broug-Holub E, Toews GB, van Iwaarden JF, Strieter RM, Kunkel SL, Paine R III, Standiford TJ. Alveolar macrophages are required for protective pulmonary defenses in murine Klebsiella pneumonia: elimination of alveolar macrophages increases neutrophil recruitment but decreases bacterial clearance and survival. Infect. Immun. 1997; 65(4):1139–1146. [PubMed: 9119443]
6. Marriott HM, Jackson LE, Wilkinson TS, Simpson AJ, Mitchell TJ, Buttle DJ, Cross SS, Ince PG, Hellewell PG, Whyte MK, Dockrell DH. Reactive oxygen species regulate neutrophil recruitment and survival in pneumococcal pneumonia. Am. J. Respir. Crit. Care Med. 2008; 177(8):887–895. [PubMed: 18202350]
7. Brown KL, Bylund J, MacDonald KL, Song-Zhao GX, Elliott MR, Falsafi R, Hancock RE, Speert DP. ROS-deficient monocytes have aberrant gene expression that correlates with inflammatory disorders of chronic granulomatous disease. Clin. Immunol. 2008; 129(1):90–102. [PubMed: 18676204]
8. Babior BM. Phagocytes and oxidative stress. Am. J. Med. 2000; 109(1):33–44. [PubMed: 10936476]
9. Andersen JK. Oxidative stress in neurodegeneration: cause or consequence? Nat. Med. 2004; (10 Suppl):S18–S25. [PubMed: 15298006]
10. Haigis MC, Yankner BA. The aging stress response. Mol. Cell. 2010; 40(2):333–344. [PubMed: 20965426]
11. Paravicini TM, Touyz RM. Redox signaling in hypertension. Cardiovasc. Res. 2006; 71(2):247–258. [PubMed: 16765337]
12. Shukla V, Mishra SK, Pant HC. Oxidative stress in neurodegeneration. Adv. Pharmacol. Sci. 2011; 2011:572634. [PubMed: 21941533]
13. Trachootham D, Alexandre J, Huang P. Targeting cancer cells by ROS-mediated mechanisms: a radical therapeutic approach? Nat. Rev. Drug Discov. 2009; 8(7):579–591. [PubMed: 19478820]

14. Karimi G, Houee Levin C, Dagher MC, Baciou L, Bizouarn T. Assembly of phagocyte NADPH oxidase: a concerted binding process? Biochim. Biophys. Acta. 2014; 1840(11):3277–3283. [PubMed: 25108064]
15. Sumimoto H. Structure, regulation and evolution of Nox-family NADPH oxidases that produce reactive oxygen species. FEBS J. 2008; 275(13):3249–3277. [PubMed: 18513324]
16. Rodaway AR, Teahan CG, Casimir CM, Segal AW, Bentley DL. Characterization of the 47-kilodalton autosomal chronic granulomatous disease protein: tissue-specific expression and transcriptional control by retinoic acid. Mol. Cell. Biol. 1990; 10(10):5388–5396. [PubMed: 2398896]
17. Lloberas J, Soler C, Celada A. The key role of PU.1/SPI-1 in B cells, myeloid cells and macrophages. Immunol. Today. 1999; 20(4):184–189. [PubMed: 10203717]
18. Bedard K, Krause KH. The NOX family of ROS-generating NADPH oxidases: physiology and pathophysiology. Physiol. Rev. 2007; 87(1):245–313. [PubMed: 17237347]
19. Ray PD, Huang BW, Tsuji Y. Reactive oxygen species (ROS) homeostasis and redox regulation in cellular signaling. Cell Signal. 2012; 24(5):981–990. [PubMed: 22286106]
20. Kaspar JW, Niture SK, Jaiswal AK. Nrf2:INrf2 (Keap1) signaling in oxidative stress. Free Radic. Biol. Med. 2009; 47:1304–1309. [PubMed: 19666107]
21. Hayes JD, Chanas SA, Henderson CJ, McMahon M, Sun C, Moffat GJ, Wolf CR, Yamamoto M. The Nrf2 transcription factor contributes both to the basal expression of glutathione S-transferases in mouse liver and to their induction by the chemopreventive synthetic antioxidants, butylated hydroxyanisole and ethoxyquin. Biochem. Soc. Trans. 2000; 28(2):33–41. [PubMed: 10816095]
22. Ishii T, Itoh K, Takahashi S, Sato H, Yanagawa T, Katoh Y, Bannai S, Yamamoto M. Transcription factor Nrf2 coordinately regulates a group of oxidative stress-inducible genes in macrophages. J. Biol. Chem. 2000; 275(21):16023–16029. [PubMed: 10821856]
23. Cho HY, Jedlicka AE, Reddy SP, Kensler TW, Yamamoto M, Zhang LY, Kleeberger SR. Role of NRF2 in protection against hyperoxic lung injury in mice. Am. J. Respir. Cell Mol. Biol. 2002; 26(2):175–182. [PubMed: 11804867]
24. Niture SK, Khatri R, Jaiswal AK. Regulation of Nrf2-an update. Free Radic. Biol. Med. 2014; 66:36–44. [PubMed: 23434765]
25. Tong KI, Padmanabhan B, Kobayashi A, Shang C, Hirotsu Y, Yokoyama S, Yamamoto M. Different electrostatic potentials define ETGE and DLG motifs as hinge and latch in oxidative stress response. Mol. Cell. Biol. 2007; 27(21):7511–7521. [PubMed: 17785452]
26. Jiang ZY, Lu MC, You QD. Discovery and development of Kelch-like ECH-associated protein 1. Nuclear factor erythroid 2-related factor 2 (KEAP1:NRF2) protein-protein interaction inhibitors: achievements, challenges, and future directions. J. Med. Chem. 2016; 59(24):10837–10858. [PubMed: 27690435]
27. Sekhar KR, Yan XX, Freeman ML. Nrf2 degradation by the ubiquitin proteasome pathway is inhibited by KIAA0132, the human homolog to INrf2. Oncogene. 2002; 21(44):6829–6834. [PubMed: 12360409]
28. Nguyen T, Sherratt PJ, Pickett CB. Regulatory mechanisms controlling gene expression mediated by the antioxidant response element. Annu. Rev. Pharmacol. Toxicol. 2003; 43:233–260. [PubMed: 12359864]
29. Chan K, Kan YW. Nrf2 is essential for protection against acute pulmonary injury in mice. Proc. Natl. Acad. Sci. USA. 1999; 96(22):12731–12736. [PubMed: 10535991]
30. Thimmulappa RK, Scollick C, Traore K, Yates M, Trush MA, Liby KT, Sporn MB, Yamamoto M, Kensler TW, Biswal S. Nrf2-dependent protection from LPS induced inflammatory response and mortality by CDDO-Imidazolide. Biochem. Biophys. Res. Commun. 2006; 351(4):883–889. [PubMed: 17097057]
31. Rangasamy T, Guo J, Mitzner WA, Roman J, Singh A, Fryer AD, Yamamoto M, Kensler TW, Tuder RM, Georas SN, Biswal S. Disruption of Nrf2 enhances susceptibility to severe airway inflammation and asthma in mice. J. Exp. Med. 2005; 202(1):47–59. [PubMed: 15998787]
32. Thimmulappa RK, Lee H, Rangasamy T, Reddy SP, Yamamoto M, Kensler TW, Biswal S. Nrf2 is a critical regulator of the innate immune response and survival during experimental sepsis. J. Clin. Investig. 2006; 116(4):984–995. [PubMed: 16585964]

33. Joo M, Kwon M, Cho YJ, Hu N, Pedchenko TV, Sadikot RT, Blackwell TS, Christman JW. Lipopolysaccharide-dependent interaction between PU.1 and c-Jun determines production of lipocalin-type prostaglandin D synthase and prostaglandin D2 in macrophages. Am. J. Physiol. Lung Cell. Mol. Physiol. 2009; 296(5):L771–L779. [PubMed: 19181746]
34. Shim G, Choi HW, Lee S, Choi J, Yu YH, Park DE, Choi Y, Kim CW, Oh YK. Enhanced intrapulmonary delivery of anticancer siRNA for lung cancer therapy using cationic ethylphosphocholine-based nanolipoplexes. Mol. Ther. 2013; 21(4):816–824. [PubMed: 23380818]
35. Han CW, Kwun MJ, Kim KH, Choi JY, Oh SR, Ahn KS, Lee JH, Joo M. Ethanol extract of Alismatis Rhizoma reduces acute lung inflammation by suppressing NF-kappaB and activating Nrf2. J. Ethnopharmacol. 2013; 146(1):402–410. [PubMed: 23333748]
36. Groemping Y, Rittinger K. Activation and assembly of the NADPH oxidase: a structural perspective. Biochem. J. 2005; 386(Pt 3):401–416. [PubMed: 15588255]
37. Jaiswal AK. Nrf2 signaling in coordinated activation of antioxidant gene expression. Free Radic. Biol. Med. 2004; 36(10):1199–1207. [PubMed: 15110384]
38. Dinkova-Kostova AT, Holtzclaw WD, Cole RN, Itoh K, Wakabayashi N, Katoh Y, Yamamoto M, Talalay P. Direct evidence that sulfhydryl groups of Keap1 are the sensors regulating induction of phase 2 enzymes that protect against carcinogens and oxidants. Proc. Natl. Acad. Sci. USA. 2002; 99(18):11908–11913. [PubMed: 12193649]
39. Klebanoff SJ. Myeloperoxidase: friend and foe. J. Leukoc. Biol. 2005; 77(5):598–625. [PubMed: 15689384]
40. Lapouge K, Smith SJ, Groemping Y, Rittinger K. Architecture of the p40-p47-p67phox complex in the resting state of the NADPH oxidase. A central role for p67phox. J. Biol. Chem. 2002; 277(12): 10121–10128. [PubMed: 11796733]
41. Groemping Y, Lapouge K, Smerdon SJ, Rittinger K. Molecular basis of phosphorylation-induced activation of the NADPH oxidase. Cell. 2003; 113(3):343–355. [PubMed: 12732142]
42. Marcoux J, Man P, Petit-Haertlein I, Vives C, Forest E, Fieschi F. p47phox molecular activation for assembly of the neutrophil NADPH oxidase complex. J. Biol. Chem. 2010; 285(37):28980–28990. [PubMed: 20592030]
43. Brown GE, Stewart MQ, Liu H, Ha VL, Yaffe MB. A novel assay system implicates PtdIns(3,4)P(2), PtdIns(3)P, and PKC delta in intracellular production of reactive oxygen species by the NADPH oxidase. Mol. Cell. 2003; 11(1):35–47. [PubMed: 12535519]
44. Faure MC, Sulpice JC, Delattre M, Lavielle M, Prigent M, Cuif MH, Melchior C, Tschirhart E, Nusse O, Dupre-Crochet S. The recruitment ofp47(−phox) and Rac2G12V at the phagosome is transient and phosphatidylserine dependent. Biol. Cell. 2013; 105(11):501–518. [PubMed: 23870057]
45. Moi P, Chan K, Asunis I, Cao A, Kan YW. Isolation of NF-E2-related factor 2 (Nrf2), a NF-E2-like basic leucine zipper transcriptional activator that binds to the tandem NF-E2/AP1 repeat of the beta-globin locus control region. Proc. Natl. Acad. Sci. USA. 1994; 91(21):9926–9930. [PubMed: 7937919]

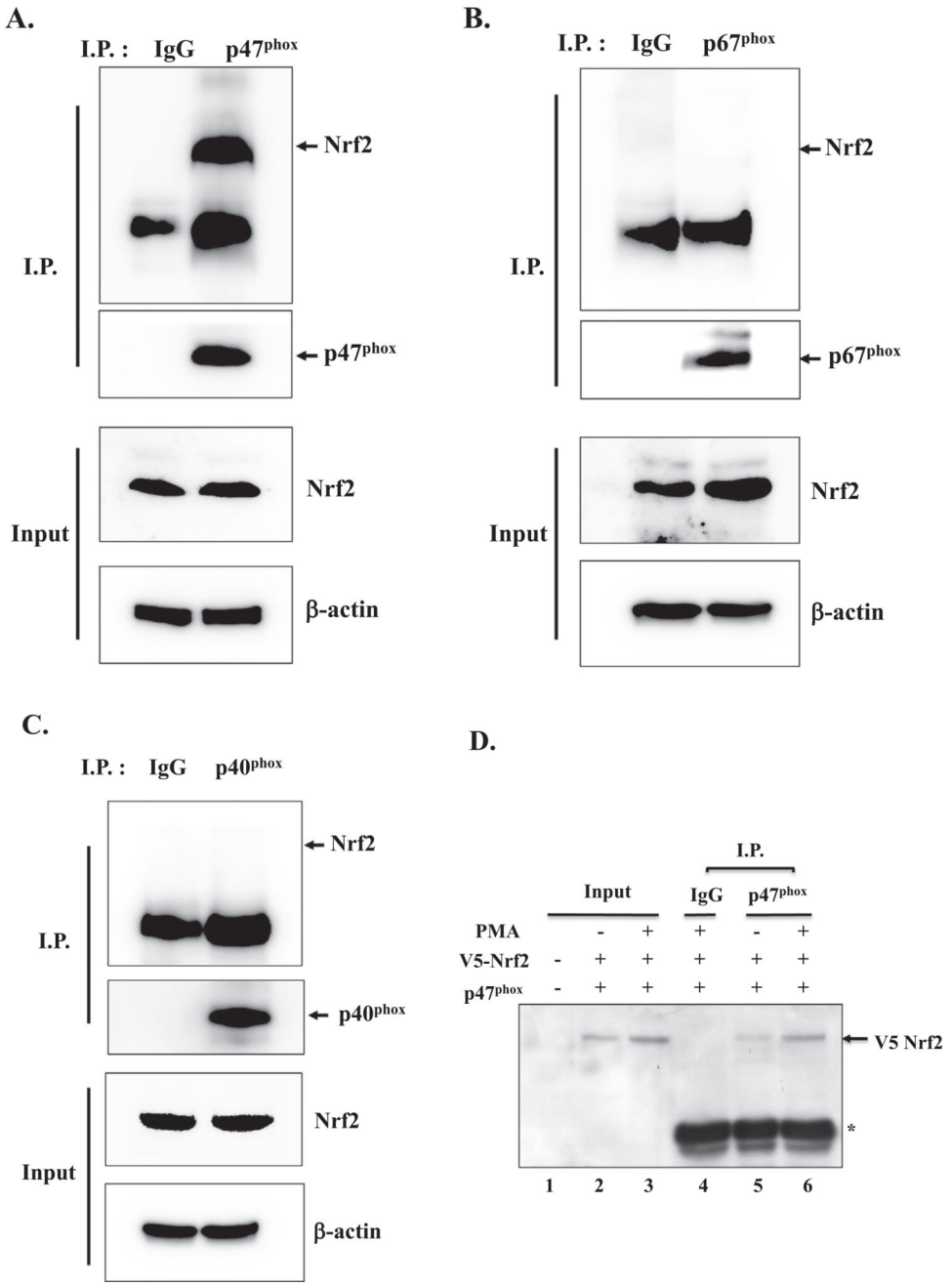

Fig. 1.

p47^{phox} physically binds to Nrf2. (A) The lysate of RAW 264.7 cells was added with the anti-p47^{phox} antibody or isotypic IgG. The precipitate of immune complex was analyzed by immunoblotting of Nrf2 to determine Nrf2 co-precipitated with p47^{phox} (top panel). The immune complex was also analyzed by immunoblotting of p47^{phox} to verify p47^{phox} precipitated by the corresponding antibody (second panel). As for input, one tenth of the cell lysate was analyzed by immunoblotting of Nrf2 (third panel) and of β-actin (bottom panel). Similar experiment was performed to determine Nrf2 co-precipitated with p67^{phox} (B) or p40^{phox} (C) with anti-p67^{phox} and anti-p40^{phox} antibodies, respectively. Arrow indicates the

putative size of Nrf2 (top panel). The precipitate of immune complex was also analyzed by immunoblotting of $p67^{phox}$ or $p40^{phox}$ (second panels in B and C). As for input, one tenth of the cell lysate was similarly analyzed by immunoblotting of Nrf2 (third panels in B and C) and of β-actin (bottom panels in B and C). (D) HEK 293 cells were transfected with the plasmids expressing V5-Nrf2 and $p47^{phox}$ in the absence (lanes 2 and 5) or presence (lanes 3 and 6) of PMA (5 μg/ml for 1 h prior to cell lysis). The cell lysate of the transfected cells was prepared for immunoprecipitation with an anti-$p47^{phox}$ antibody or isotypic IgG. The immune complex was analyzed by immunoblotting for V5 (Nrf2). * indicates the heavy chain of added antibodies.

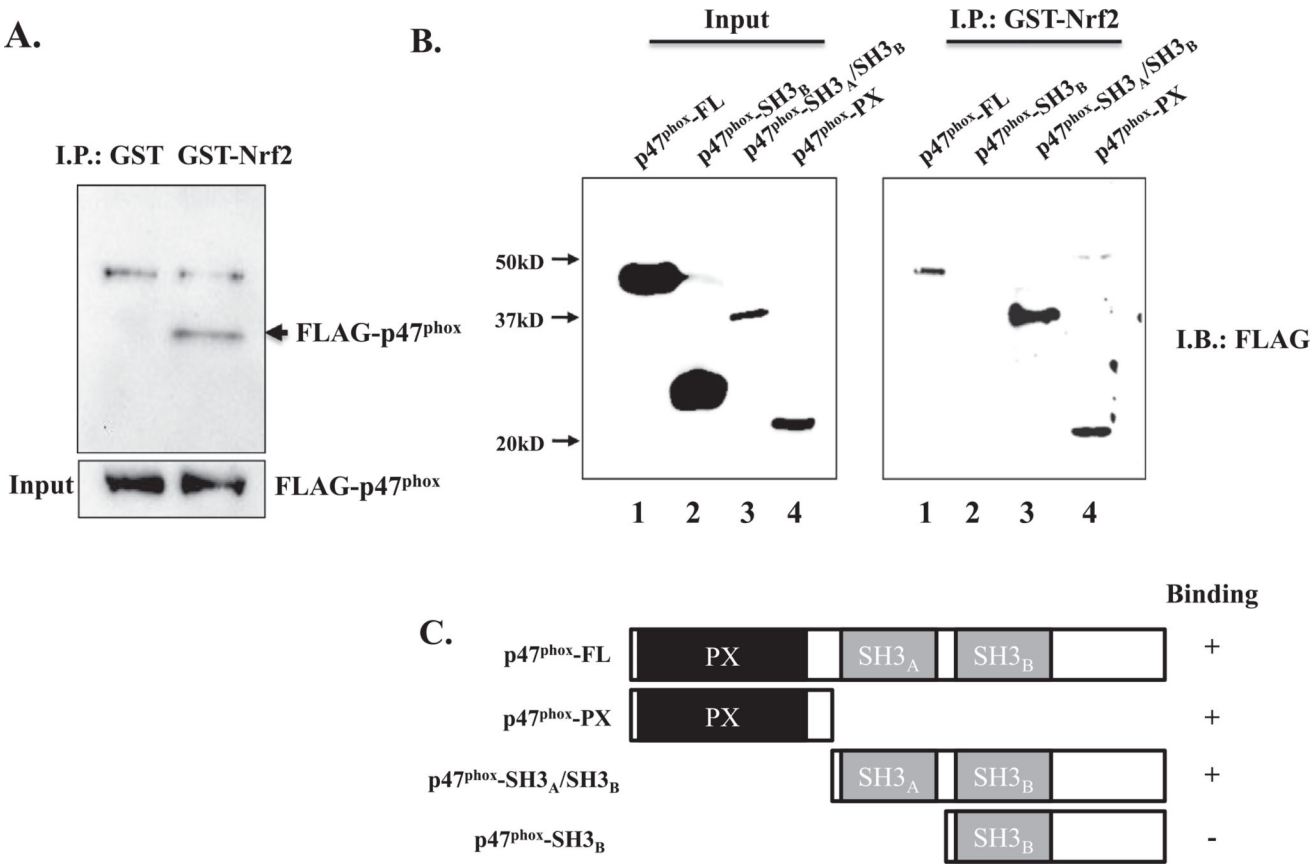

Fig. 2.

The PX and $SH3_A$ domains of $p47^{phox}$ are important in binding to Nrf2. (A) GST-fused Nrf2 expressed in *E.coli.* was captured by GSH-agarose beads, the complex of which was incubated with the lysate of HEK 293 cells that were transfected with the plasmid expressing FLAG-tagged $p47^{phox}$. Western blot was performed with an anti-FLAG antibody to reveal $p47^{phox}$ proteins bound to GST-Nrf2. As for input, one tenth of the transfected cell lysate was analyzed by immunoblotting of FLAG-$p47^{phox}$ (second panel). (B) A similar experiment was performed with various deletion mutants of $p47^{phox}$. The GST-Nrf2 beads were incubated with the cell lysate containing the FLAG-tagged full-length $p47^{phox}$ ($p47^{phox}$-FL) or FLAG-tagged mutants of $p47^{phox}$ that have the PX domain ($p47^{phox}$-PX), tandem SH3 domains and C-terminus ($p47^{phox}$-$SH3_A/SH3_B$), or $SH3_B$ domain and C-terminus ($p47^{phox}$-$SH3_B$) of $p47^{phox}$. Western blot was performed with an anti-FLAG antibody to reveal any mutants of $p47^{phox}$ bound to GST-Nrf2. One tenth of the transfected cell lysate was used for input. The summary of the binding between the mutants and Nrf2 was shown in (C).

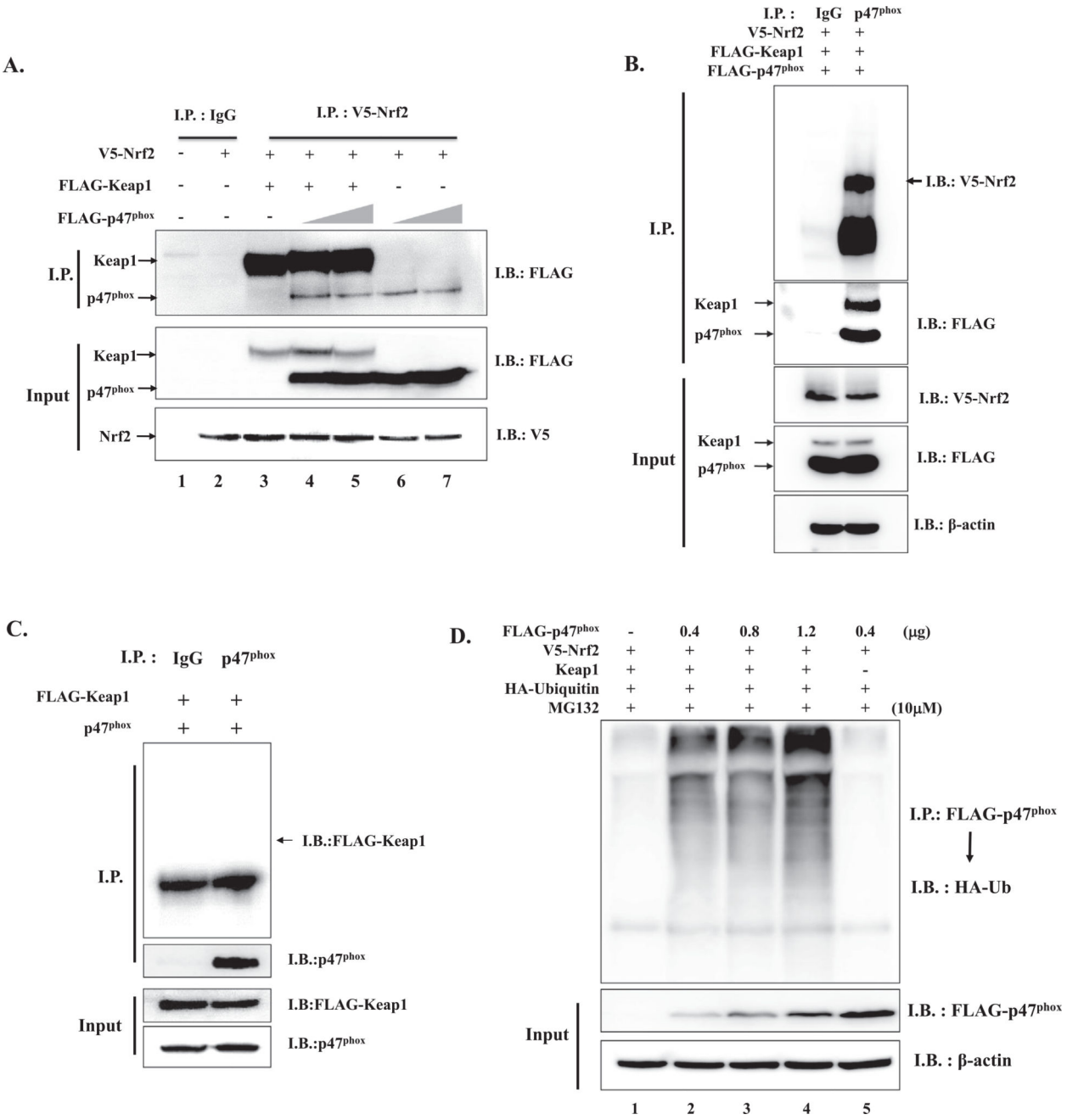

Fig. 3.

p47^{phox} binding to Nrf2/Keap1 complex results in ubiquitinated p47^{phox}. (A) HEK 293 cells were transfected with the plasmids encoding V5-Nrf2, FLAG-Keap1, and FLAG-p47^{phox}, and 48 h after transfection the cytosolic fractions of the transfected cells were prepared for immunoprecipitation with an anti-V5 antibody or isotypic IgG. The proteins co-precipitated with the anti-V5 antibody (V5-Nrf2) were revealed by immunoblotting for FLAG (Keap1 and p47^{phox}; top panel). As for input, one tenth of the cell lysate was similarly analyzed by immunoblotting for FLAG-tagged proteins (Keap1 and p47^{phox}; second panel) or V5-tagged protein (Nrf2; bottom panel). (B) HEK 293 cells were similarly transfected with the

plasmids encoding V5-Nrf2, FLAG-Keap1, and FLAG-p47^{phox}, and immunoprecipitation was performed with an anti-p47phox antibody or isotypic IgG. The proteins co-precipitated with the anti-p47^{phox} antibody were revealed by immunoblotting for V5 (Nrf2; top panel) and FLAG (Keap1 and p47^{phox}; top panel). As for input, one tenth of the cell lysate was similarly analyzed by immunoblotting for V5 (Nrf2; third panel) and FLAG (Keap1 and p47phox, fourth panel; β-actin, bottom panel). (C) From HEK 293 cells transfected with the plasmids encoding p47^{phox} and FLAG-Keap1, p47^{phox} was precipitated with the anti-p47^{phox} antibody (second panel). Keap1 associated with p47^{phox} was revealed by the anti-FLAG antibody (arrow in the top panel). As for input, one tenth of the cell lysate was similarly analyzed by the anti-FLAG for FLAG-tagged Keap1 (third panel) or anti-p47^{phox} antibody (bottom panel). (D) HEK 293 cells were transfected with the indicated amounts of plasmids encoding FLAG-p47^{phox}, V5-Nrf2, Keap1, and HA-Ub, to which MG132 (10 μM) was added 3 h prior to cell lysis. FLAG-p47^{phox} was precipitated with the anti-FLAG antibody, and the status of ubiquitination of p47^{phox} was revealed by immunoblotting of HA-Ub (top panel). As for input, one tenth of the transfected cell lysate was similarly analyzed by immunoblotting of FLAG-p47^{phox} (second panel) and β-actin (bottom panel).

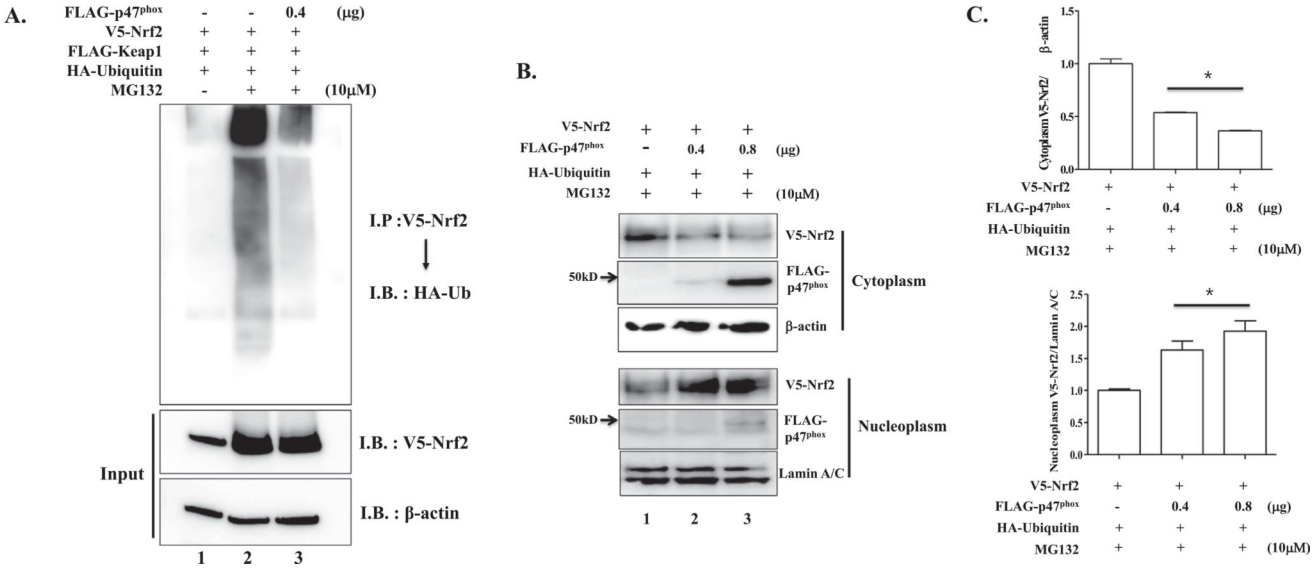

Fig. 4.

p47^{phox} suppresses the ubiquitination of Nrf2 and increases the nuclear Nrf2. (A) HEK 293 cells were transfected with the plasmids encoding V5-Nrf2, FLAG-Keap1, HA-Ub, and FLAG-p47^{phox}, with or without MG132. V5-Nrf2 was precipitated and the status of the ubiquitination of Nrf2 was revealed by subsequent immunoblotting of HA-Ub (top panel). One tenth of the transfected cell lysate was similarly analyzed by immunoblotting of V5-Nrf2 (second panel) and β-actin (bottom panel). (B) HEK 293 cells were transfected with the plasmids encoding V5-Nrf2, HA-Ub, and FLAG-p47^{phox}, with MG132. The cytoplasmic and nuclear fractions of the transfected cells were prepared and analyzed by immunoblotting of V5-Nrf2 (top panels) and FLAG-p47^{phox} (second panels), along with internal controls for cytoplasmic (β-actin) and nuclear proteins (lamin A/C). (C) The relative expression of Nrf2 over β-actin in the cytosol or laminA/C in the nucleus was measured by ImageJ. Results represent the mean ± SEM of three independent measurements. *P was less than 0.05, compared to V5-Nrf2 without p47^{phox}.

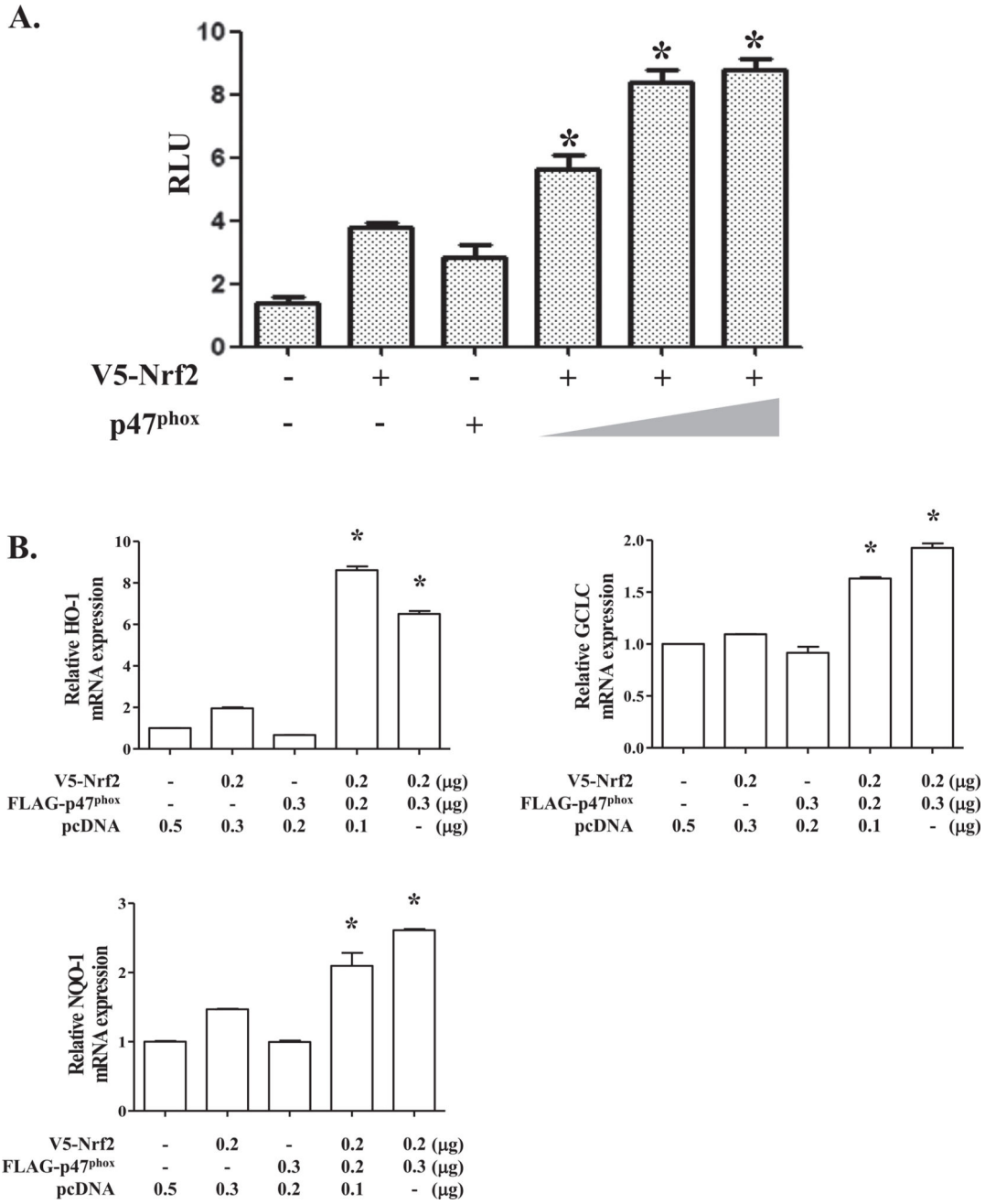

Fig. 5.

p47^{phox} enhances the transcriptional activity of Nrf2. (A) Luciferase reporter assay was performed to measure Nrf2 transcription activity. A reporter cell line derived from RAW 264.7 cells that were stably transfected with a Nrf2-driven luciferase reporter construct, were transfected with a fixed amount of the plasmid encoding Nrf2 (0.2 μg) and increasing amounts of the plasmid encoding p47^{phox} (0.2, 0.3, and 0.5 μg) for 48 h. The amount of transfected plasmids was adjusted to 0.7 μg in total with an empty vector. The assay was performed in triplicate, and the luciferase activity was normalized by the amount of total proteins. The mean ± SEM of three independent measurements is shown in relative

luciferase unit (RLU). *P was less than 0.01, compared with the control transfected with V5-Nrf2 only. (B) HEK 293 cells were transfected with the Nrf2 and $p47^{phox}$ expressing plasmids for 48 h. The mRNA of Nrf2-dependent genes, such as HO-1, GCLC, and NQO-1, was analyzed by a real-time qPCR. As for internal controls, GAPDH mRNA was similarly analyzed. A similar experiment was repeated at least three times, and representative results are shown. Results represent the mean ± SEM of triplicate measurement. *P was less than 0.05, compared with the transfected with V5-Nrf2 only.

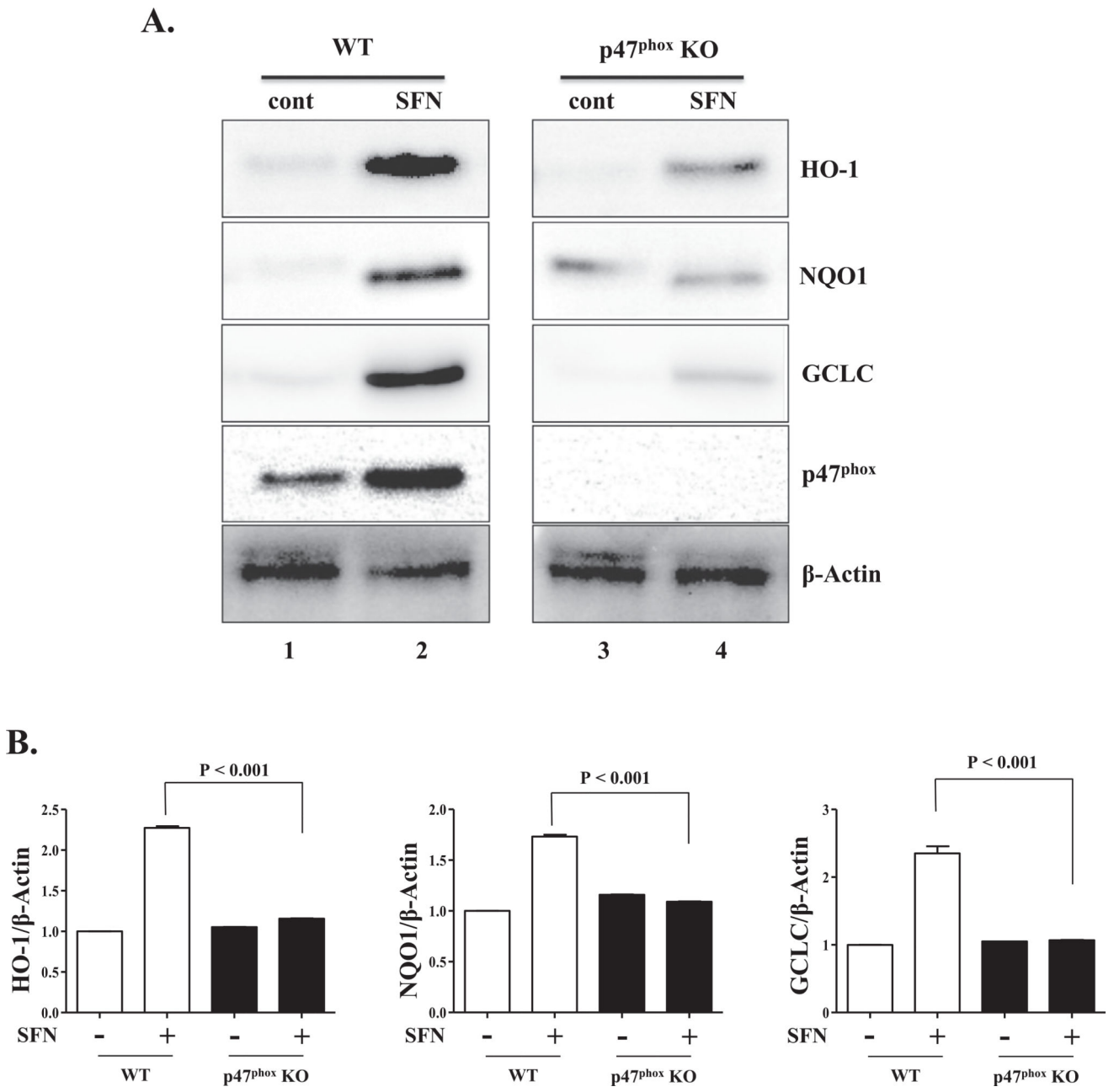

Fig. 6.

Genetic ablation of p47^{phox} decreases the expression of Nrf2-dependent genes. (A) BMDM were prepared from wild-type (WT) and p47$^{phox-/-}$ mice (KO). The levels of Nrf2-dependent gene products including HO-1 (first panel), NQO-1 (second panel), and GCLC (third panel) in BMDM of WT were compared with those of p47^{phox} KO mice by western blot analysis. The membrane was stripped and reprobed for β-actin. A similar experiment was performed at least three times independently. Representative results are shown. (B) Relative expression of each protein over β-actin is shown after each band was quantitated by ImageJ. Results represent the mean ± SEM of three independent measurements. Expressions

of Nrf2-dependent gene products were significantly decreased in BMDM of $p47^{phox}$ KO mice, compared to WT ($P < 0.001$).

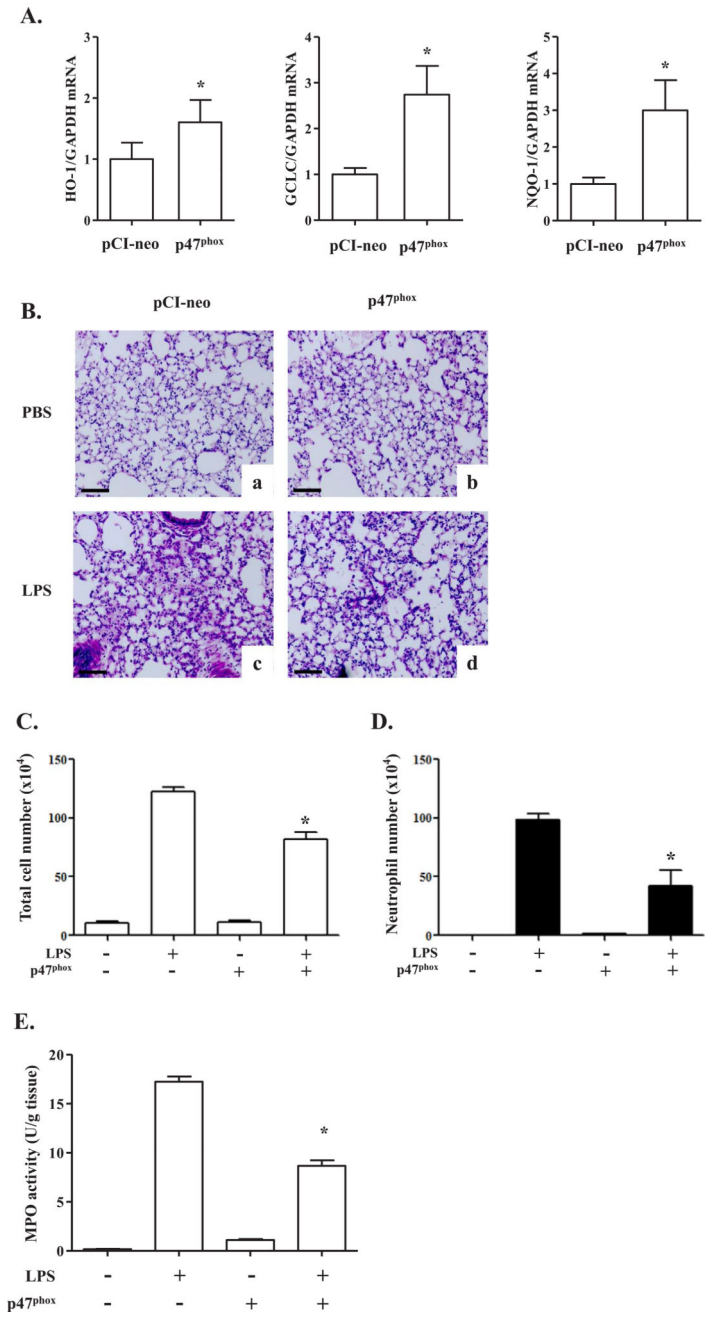

Fig. 7.

Selective expression of p47^{phox} in mouse lungs induces Nrf2-dependent gene expression and protects mice from neutrophilic lung inflammation induced by LPS. (A) C57BL/6 mice (n = 5 per group) received intratracheal (i.t.) delivery of host vector (pCI-neo) or the p47^{phox} expressing vector. At 48 h after the administration of the plasmid, mouse lungs were harvested, and total RNA was isolated for the semi-quantitative RT-PCR analysis of Nrf2-dependent genes. Relative expression of each mRNA of the genes over GAPDH was quantitated by ImageJ. Representative results are shown in the mean ± SEM of five mouse lungs. *P was less than 0.05, compared with vector-treated mice. (B) C57BL/6 mice (n = 5

per group) received similarly pCI-neo (a, c) or the $p47^{phox}$ expressing vector (b, d). At 48 h after the administration, mice were treated with an intraperitoneal (i.p.) PBS (a, b) or LPS (c, d). At 16 h after the treatment, mouse lungs were harvested for histologic analysis. Lung sections were HE stained for histological examination (magnification ×100). Shown are representatives of at least five different areas of a lung (bar = 50 μm). BAL was performed for counting total cells (C) and neutrophils (D) in the lungs of the mice. Similarly, MPO activity of neutrophils in the lung was measured (E). Data represent the mean± SEM of three independent measurements. *P was less than 0.05, compared with LPS-treated mice.